

# Analysis of Crystals Leading to Joint Arthropathies by Raman Spectroscopy: Comparison with Compensated Polarized Imaging

XINGGUO CHENG, DONARD G. HAGGINS, RUSSEL H. YORK, YENER N. YENI,  
and OZAN AKKUS\*

*Weldon School of Biomedical Engineering, Purdue University, West Lafayette, Indiana 47907 (X.C., O.A.); Department of Rheumatology, Henry Ford Hospital, 24555 Haig, Taylor, Michigan 48180 (D.G.H.); Beale Institute, 4333 W Joe Hwy #1, Lansing, Michigan 48917 (R.H.Y.); and Bone and Joint Center, Department of Orthopaedics and Rehabilitation, Henry Ford Hospital, 2799 West Grand Boulevard, Detroit, Michigan 48202 (Y.N.Y.)*

The current study assessed the feasibility of the application of Raman spectroscopy toward the diagnosis of gout and pseudogout. First, the lowest concentrations of monosodium urate monohydrate (MSUM) and calcium pyrophosphate dihydrate (CPPD) crystals detectable by Raman spectroscopy were investigated by mixing known amounts of synthetic crystals with synovial fluid in the concentration range of 1 to 100  $\mu\text{g/mL}$ . Second, a digestion protocol was developed for clinical samples to improve crystal extraction. The ensuing centrifugation of the digest congregated crystals at a well-defined point and allowed for point-and-shoot Raman analysis without having to conduct an extensive search for individual crystals. Finally, synovial fluid samples obtained from patients ( $n = 35$ ) were cross-analyzed by polarized light microscopy (PLM) and the Raman method to compare and contrast the diagnoses of the two methods. It was found that Raman spectroscopy can detect MSUM and CPPD crystals with good sensitivity and specificity at concentrations as low as 5  $\mu\text{g/mL}$  and 2.5  $\mu\text{g/mL}$ , respectively, using the current method. This detection limit of Raman analysis is lower than that reported for PLM. Raman and PLM diagnoses of clinical samples agreed in 32 out of 35 samples in the entire sample pool. However, the rate of disagreement between PLM-based and Raman-based diagnoses was noteworthy within the subset of diseased samples (3 out of 10), indicating that PLM has limitations and that the confirmation by a secondary method is essential for a reliable outcome. The proposed protocol of sample preparation and Raman analysis ascribes baseline feasibility to the diagnosis of gout and pseudogout by Raman spectroscopy, thus justifying further studies using a larger clinical sample set for obtaining sensitivity and specificity.

Index Headings: Synovial fluid; Gout; Raman spectroscopy.

## INTRODUCTION

Correct identification of monosodium urate (MSUM) and calcium pyrophosphate (CPPD) crystals is important for proceeding with the appropriate course of treatment for joint arthropathies. Ruling out the involvement of certain crystals also allows for focusing on other forms of joint diseases such as osteoarthritis or rheumatoid arthritis. The most common technique for identification of CPPD and MSUM crystals is compensated polarized light microscopy (PLM).<sup>1</sup> Sample handling is easy and a microscope equipped with the appropriate polarization optics is sufficient to execute the

PLM-based diagnosis. However, the procedure is affected by subjectivity such that comparison of the same sample set between different labs, or by multiple observations in the same lab, revealed significant variations in diagnosis.<sup>2–5</sup> Another difficulty in identifying crystals is when they are present at low concentrations or when their size is small.<sup>6,7</sup> There are reports on the limitations of PLM in identifying small MSUM and CPPD crystals that are known to be present as confirmed by electron microscopy.<sup>8</sup> Therefore, the threshold concentration of MSUM and CPPD crystals in synovial fluid that can be reliably detected by PLM was cautiously declared to be in the range of 10 to 100  $\mu\text{g/mL}$ .<sup>7</sup> Crystals that do not display positive or negative birefringence cannot be detected by PLM, making PLM limited to identifying MSUM and CPPD. For instance, amorphous intracellular basic calcium phosphates (BCP) require alizarin red staining for identification.<sup>9</sup> Non-birefringent or weakly birefringent crystals (such as calcium phosphate), intracellular crystals, or crystals with smaller size (less than 2  $\mu\text{m}$  such as hydroxyapatite) may elude identification since PLM determination is totally dependent on interference color and crystal shape.<sup>10</sup> Such limitations in sensitivity and repeatability of PLM may have negative repercussions on the ensuing clinical treatment.<sup>11</sup> Therefore, it is important to find alternative or complementary analytical techniques for unequivocal identification of crystals. Raman spectroscopy can be useful toward this end.

McGill et al. identified gout crystals in a synovial smear and a gouty tophus from a limited number of clinical samples using Raman analysis.<sup>12</sup> Maugars et al. observed CPPD crystals in cartilage, muscle, and tendon sections using Raman microscopy.<sup>13</sup> Hawi et al. have identified cholesterol crystals within cells resident in synovial aspirates.<sup>14</sup> However, these studies utilized Raman spectroscopy in the microscopy mode, which requires seeking for individual crystals visually, a common strategy with PLM. This approach is limited in identifying smaller crystals or crystals present at low concentrations. Therefore, there is a need to develop sample preparation techniques that will congregate crystals at well-defined locations and target them in the point-and-shoot mode without having to survey for individual crystallites. The large amount of organic debris present in the synovial fluid of arthritis patients is another critical aspect associated with sample

Received 22 October 2008; accepted 5 January 2009.

\* Author to whom correspondence should be sent. E-mail: ozan@purdue.edu.

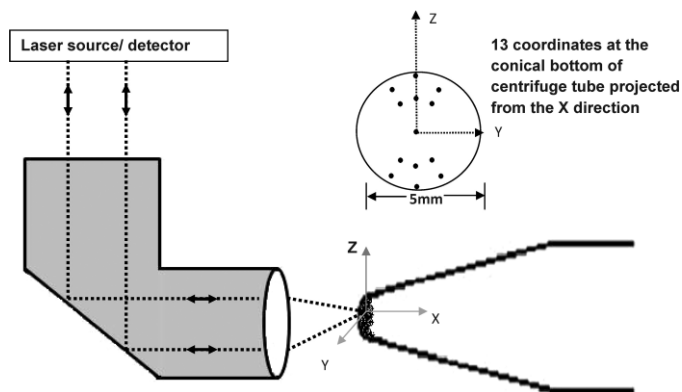


FIG. 1. Schema of the 13-point Raman detection at the conical bottom of the centrifuge tube, which contains crystal pellets. The incidence laser from the macrolens in the  $x$ -direction was focused on the sample at the specific  $y,z$ -coordinate. Scattered photons were collected by the sample lens and transferred to the detector to record the Raman spectrum. The total intensity of major Raman peaks was summed over the 13 points to obtain an estimate of the amount of crystal present.

preparation. Therefore, the proper sample preparation procedure for Raman spectroscopy should also reduce the organics without dissolution of existing crystals or formation of artifactual crystals.

Other missing critical information on Raman-based diagnosis of MSUM and CPPD are the detection thresholds for crystal concentration and the ability to measure the amount of crystals. Clinically, crystals are observed in the range of 10 to 100  $\mu\text{g}/\text{mL}$ ;<sup>7</sup> whether or not Raman analysis can converge the lower end of this range remains to be determined.

The first aim of the current study was to develop a synovial aspirate sample preparation method that will allow the identification of crystal type, amount, and detection threshold using a point-and-shoot Raman laser spectroscopy approach. The second aim was to compare the Raman-based diagnosis from clinical samples prepared as such to the PLM-based diagnosis.

## EXPERIMENTAL

MSUM and CPPD were synthesized following earlier protocols<sup>15,16</sup> that yield crystals with similar size, morphology, and birefringence to those found in gout and pseudogout.<sup>17</sup> Raman analysis of all samples was performed using a Raman microscope (Labram HR800, Horiba Jobin Yvon, Edison, NJ). The system consists of a laser source at 660 nm, and measurements were performed using a 600 lines/mm grating, which provided a spectral dispersion of 1.25 pixels/ $\text{cm}^{-1}$ . The device is equipped with a three-dimensional (3D) mapping stage, which allows the laser to be positioned on the sample. The Raman wavenumber shift measured by the system was calibrated using the known 520.7  $\text{cm}^{-1}$  peak of a Si wafer. Measurements were taken by using a 10 $\times$  objective and the final spectrum was obtained as the average of five consecutive spectra, each collected for 5 s.

Synovial fluid was obtained from donors with no known history of joint disease from the National Disease Research Interchange (NDRI, Philadelphia, PA). In order to prevent crystal dissolution while achieving the correct concentration, synovial fluid was digested serially and centrifuged as per the protocol laid out later. Half a milliliter (0.5 mL) of synovial fluid was loaded in glass centrifuge tubes (Corning, 8060–15,

NY) and 0.3 mg of lyophilized hyaluronidase powder (Sigma, H3506) was added. After 15 min digestion at room temperature, the solution was centrifuged at 4000 rpm for 15 min. The supernatant in each tube was discarded. The pellet in each tube was mixed with 0.5 mL MSUM solution (prepared by dispersing MSUM crystal in filtered MSUM-supersaturated solution) at six different concentrations (1, 2.5, 5, 10, 20, and 100  $\mu\text{g}/\text{mL}$ ). Half a milligram (0.5 mg) of lyophilized papain powder (Sigma, P4762) was added to each crystal-containing tube. The above solution was incubated at 37  $^{\circ}\text{C}$  for 30 min and then centrifuged again at 4000 rpm for 15 min. The supernatant was discarded. The glass tubes containing the dried pellets were further dried at 50  $^{\circ}\text{C}$  and used for Raman detection. A similar procedure as described above was also used for CPPD crystals.

Following centrifugation, MSUM or CPPD crystals were aggregated at the bottom tip of the conical glass tubes over a circular area with a diameter of about 2 mm. The distribution of crystals was random over this area. We did not employ the optical microscope feature of the device since our aim was to congregate crystals at a well-defined location, thereby eliminating the need for visual confirmation of the presence of crystals at the observation point. Rather, thirteen points with predefined coordinates (Fig. 1) were decided upon and the laser was manually focused at these points without any visual confirmation of the presence of crystals. The number of points was determined by analyzing sets of different numbers of measurements and 13 points provided a reasonable standard deviation (less than 15% of mean).

The MSUM crystals were identified by their characteristic peak at 631  $\text{cm}^{-1}$ , which originates from the vibrations of the purine ring,<sup>18</sup> whereas, the CPPD crystals were identified from the peak at 1049  $\text{cm}^{-1}$  originating from the P–O stretch.<sup>19</sup> So as to obtain a Raman-based score for the amount of crystals, summation of the intensities of these peaks was taken over the thirteen observation points. Highly concentrated samples led to the outcome of crystal presence at a greater number of points and at greater density per point, generating a greater summation value. Each sample was measured three times, each time with the sample being repositioned in a different way. The total Raman intensity of each sample was plotted against the known concentration of CPPD or MSUM applied to the synovial fluids to find the relationship between the two. The significance of the linear regression was determined by Minitab software at the level of  $P < 0.05$ .

Under informed consent approved by the Institutional Review Boards of both participating institutions, synovial fluid samples were collected from patients who were undergoing a routine sterile intraarticular joint aspiration. Samples were collected on a first-come first-served basis regardless of age, gender, and race. Each of the 35 synovial fluid samples was divided into two parts. One part was sent to Pathology, as is routinely done, for crystal identification by PLM. The remainder of the sample (up to 5 mL) was placed in a sealed sterile container, labeled with a code number, and transferred overnight on dry ice to the Orthopaedic Bioengineering Laboratories at Purdue University. These clinical synovial fluid samples were immediately placed in a freezer dedicated for storage of human tissue samples and kept at  $-40^{\circ}\text{C}$  until used for Raman analysis. The outcome of the clinical PLM diagnosis was not revealed to the researchers conducting the Raman analysis (X.C., O.A.) until after the completion of the Raman studies, with the exception of four clinical samples that were

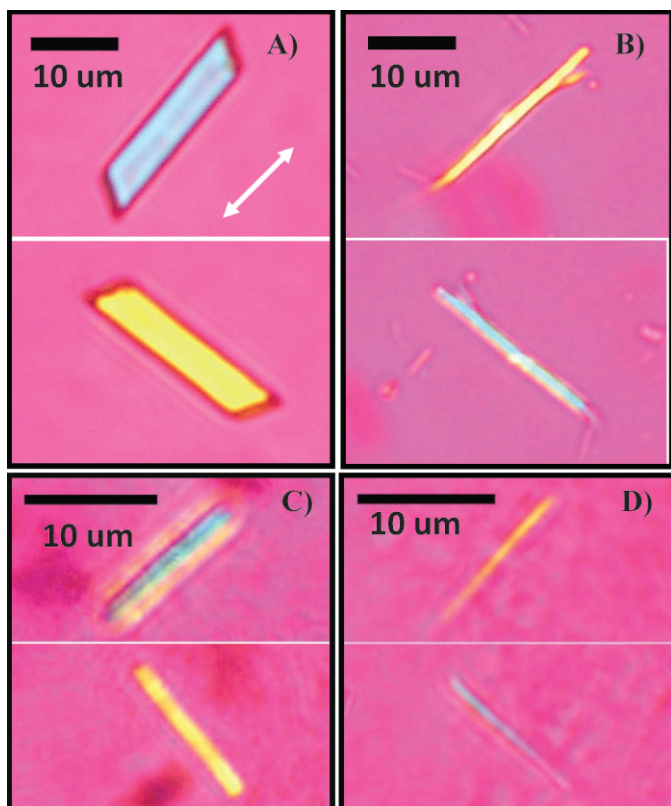


FIG. 2. Compensated polarized optical images of CPPD and MSUM crystals. (A, B) Synthetic CPPD and MSUM crystals suspended in synovial fluid viewed from  $0^\circ$  and  $90^\circ$  to the slow axis (denoted by white double arrow) of the gypsum plate. (C, D) Clinical pseudogout and gout samples.

used for testing the digestion procedure, which were developed earlier using mixtures of synovial fluid and synthetic crystals.

For each clinical sample, 4 mL of synovial fluid was loaded in the centrifuge tubes. A hyaluronidase digestion procedure similar to that described earlier was followed. The tubes were then centrifuged at 4000 rpm for 15 min and 3.5 mL of the supernatant was removed, leaving 0.5 mL of liquid. The pellet was re-dispersed in the remaining liquid. Four milligrams (4 mg) of papain powder and 0.08 g of sodium dodecyl sulfate powder (SDS, Mallinckrodt Baker, Inc., Phillipsburg, NJ) were added and the mixture was kept for 12 h at  $37^\circ\text{C}$ . SDS was added to facilitate digestion of lipid cell membranes and increase efficacy of papain to digest cytoplasmic material, in turn releasing intracellular crystals. After digestion, the tubes were centrifuged at 4000 rpm for 15 min, supernatants were removed, and the pellet was retained for Raman analysis.

Raman analysis for the identification of crystals in the clinical samples was performed by acquiring signals directly from the birefringent regions in the pellet. At least five spectra were recorded per aspirate. The presence of a peak at  $631\text{ cm}^{-1}$  and a peak at  $1049\text{ cm}^{-1}$  were taken as the Raman-based diagnosis criteria for gout and pseudogout, respectively. The samples diagnosed with the presence of crystals were also analyzed using the thirteen-point Raman analysis described earlier to predict the amount of crystals. The crystal concentration was calculated by using the relationship between total Raman intensity and crystal concentration obtained from the previous synthetic crystal study.

## RESULTS

Compensated polarized light microscopic analysis of the synthetic MSUM and CPPD crystals confirmed that these crystals have shape and dimensions comparable to those observed clinically and with the expected type of birefringence (Fig. 2). Synthetic MSUM crystals displayed the typical needle shape observed in the clinical setting. The average length of synthetic MSUM needles was  $14 \pm 9\text{ }\mu\text{m}$  with the range of length varying from 5 to  $50\text{ }\mu\text{m}$ , a range slightly larger but comparable to that reported clinically.<sup>20</sup> CPPD crystals were rhomboid or rod-shaped. The average length of CPPD crystals was  $13 \pm 6\text{ }\mu\text{m}$ , the length ranging from 4 to  $27\text{ }\mu\text{m}$ . Therefore, the key qualities of synthetic crystals were similar to those commonly found *in vivo*.

The Raman spectrum (Fig. 3A, middle) recorded from synthetic MSUM had the most intense peak appear at  $631\text{ cm}^{-1}$ . The spectrum of synthetic CPPD (Fig. 3A, bottom) displayed the strongest peak around  $1050\text{ cm}^{-1}$  (symmetric vibration of  $\text{PO}_3$ ). The spectra of both synthetic crystals were in agreement with those recorded from purified biological samples in this study as well as those reported by others earlier.<sup>12</sup> Hydroxyapatite (HA) is a relatively rarely observed crystal in the synovial fluid. The Raman spectrum of HA had its strongest peak around  $960\text{ cm}^{-1}$  and did not overlap with major peaks of either MSUM or CPPD (Fig. 3A, top).

Typical Raman spectra from clinical samples containing MSUM or CPPD crystals displayed the expected characteristic peaks (Fig. 3B). For normal synovial fluid samples, no characteristic peaks were observed (Fig. 3B bottom).

The summation of the intensities of characteristic Raman peaks over the thirteen observation points was significantly and linearly related to the known crystal concentration (for MSUM,  $R^2 = 0.986$ ,  $P < 0.05$  and for CPPD,  $R^2 = 0.995$ ,  $P < 0.05$ , Figs. 3C and 3D). Using the 13-point method, Raman spectroscopy was able to detect MSUM crystals at concentrations at and above  $5\text{ }\mu\text{g/mL}$ , while it detected CPPD crystals at concentrations as low as  $2.5\text{ }\mu\text{g/mL}$ .

It was difficult to diagnose a non-treated clinical sample by PLM because the crystals were mostly intracellular (Fig. 4A). After digestion of this clinical sample, many needle-shaped birefringent crystals were revealed in the dark-field microscope image and diagnosis could be easily made from PLM (Fig. 4B).

Over the entire sample pool (normal and diseased), the diagnosis by Raman spectroscopy was in agreement with the diagnosis of an independently conducted PLM analysis for 32 out of 35 clinical samples (Table I). However, for the diseased samples only, there was agreement in 7 out of 10 samples, indicating a 30% mismatch between the two methods. In the 32 samples for which both diagnoses were the same, there were 5 gout samples and 2 pseudogout samples, and 25 samples were diagnosed to be absent of both MSUM and CPPD.

The three diseased samples with different diagnoses were re-examined by both PLM and Raman more closely for a second time. The first PLM-based clinical diagnosis of CPPD for sample 39 (Table I) was likely incorrect as the secondary PLM analysis confirmed the plate-shaped crystals with an interference color opposite to that of CPPD. Secondary Raman analysis indicated these crystals to be neither MSUM nor CPPD because no characteristic peaks were observed. Further analysis using energy dispersive X-ray spectroscopy (EDX) showed that there were neither Ca nor Na peaks on the plate-

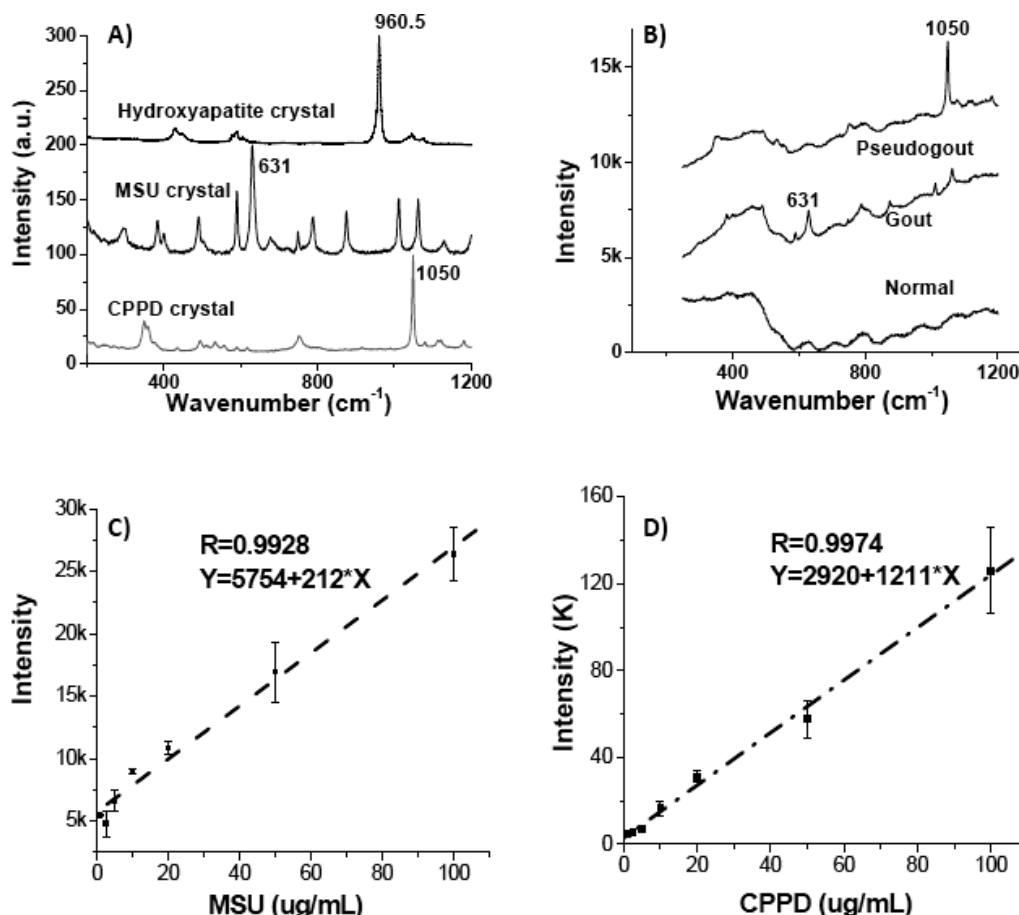


FIG. 3. Raman spectra of different samples and the 13-point analysis of Raman intensity and crystal concentration. (A) Typical Raman spectra of pure synthetic MSUM and CPPD crystals. (B) Typical Raman spectra of a gout sample, a pseudogout sample, and a normal sample after digestion and centrifugation. (C, D) The 13-point Raman analysis on the dried pellet reveals a linear relationship between the Raman intensity and crystal concentration (MSUM or CPPD) in synovial fluid.

shaped crystals. Clinical sample 16 was diagnosed as normal by the clinical PLM analysis; however, Raman diagnosis was gout. The second PLM analysis of both the original sample and the digested sample indicated that the Raman diagnosis was correct. In clinical sample 2, initial PLM analysis indicated gout, whereas the Raman diagnosis was pseudogout. The secondary analyses by both PLM and Raman revealed this

sample to contain both MSUM and CPPD crystals. Therefore, in this occasion Raman analysis missed gout whereas PLM missed pseudogout.

The 13-point analysis of clinical samples indicated that MSU crystal concentration in gouty samples was typically in the range of 5–137  $\mu\text{g/mL}$ , while CPPD crystal concentration in pseudogout samples was typically in the range of 5–27  $\mu\text{g/mL}$ .

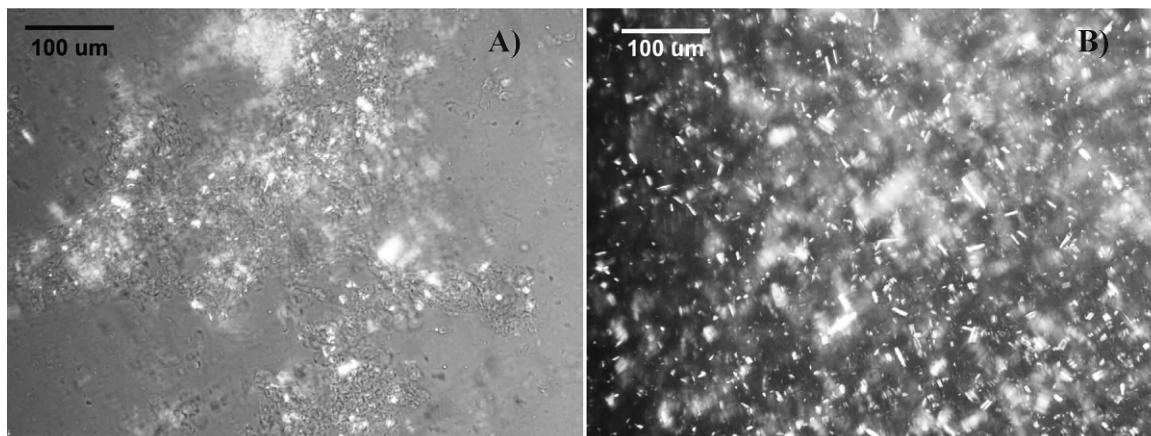


FIG. 4. The effect of digestion on the PLM analysis of a clinical sample containing MSUM crystals. (A) The dark-field image of synovial fluid without digestion showing that crystals were obscured by debris. (B) Numerous needle-shaped MSUM crystals emerged in the dark-field image following digestion.

**TABLE I.** Comparison of the diagnosis results of clinical samples based on PLM and Raman spectroscopy. PLM 1 and Raman 1 indicate the initial diagnosis conducted by the two methods with the researchers conducting analyses blinded to the results of the other one. The three samples for which the initial diagnosis was in disagreement were reevaluated and the results are shown in PLM 2 and Raman 2. When diagnoses agreed between PLM 1 and Raman 1, secondary measurements were not carried out (NA: not applicable).

Sample ID	PLM 1	Raman 1	PLM 2	Raman 2
3, 4, 5, 6, 11, 12, 13, 14, 15, 17, 18, 22, 23, 24, 25, 27, 28, 29, 30, 32, 34, 35, 36, 37, 38	Normal	Normal	NA	NA
1, 7, 10, 19, 21, 31	Gout	Gout	NA	NA
26	Pseudogout	Pseudogout	NA	NA
2	Gout	Pseudogout	Both	Both
16	Normal	Gout	Gout	Gout
39	CPPD	Normal	Normal	Normal

## DISCUSSION

In the current study, the minimum detectable crystal concentration by Raman analysis was determined for MSUM and CPPD crystals. A new digestion method was used to process the clinical synovial aspirates, which improved the Raman signal from crystals. Centrifugation of the digest congregated crystals at the bottom of centrifuge tubes within a 2 mm diameter spot, making it easier to locate crystals for analysis. Raman spectra were then acquired from clinical samples and compared to the diagnosis obtained from PLM analysis conducted in the pathology lab.

The current sample preparation method increased the time to diagnosis because of additional digestion and centrifugation steps; however, it also recovered crystals encapsulated by cellular material and concentrated crystals to well-defined locations, which in turn reduced the search time. For the sake of making the correct diagnosis, the additional sample digestion processes are justifiable. Others have proposed similar digestion procedures using mostly enzymes digesting protein and hyaluronic acid. The protocol developed in this study introduced a detergent treatment stage, which likely improved efficiency by removing cell membrane.

Our results indicate that the detection limit of Raman analysis is lower than that of PLM. This would in turn improve the sensitivity and allow earlier detection of the disease. Also, the Raman method was able to measure the amount of crystals. This ability would confirm the progression of healing as per reduced amount of crystal concentration in repeated aspirates of patients undergoing treatment. We believe that the detection threshold can be further improved by increasing the number of observation points. The convex bottom of the centrifuge tubes required manual focusing; therefore, the number of observations was limited to thirteen points, a limit that provided a reasonable coefficient of variation. The convex geometry may have reduced signal focusing and collection efficiency as well. This limitation can be addressed in the future by using glass tubes with flattened bottoms in order to increase the number of observations and decrease the detection threshold further.

Raman analysis can provide definitive diagnosis of gout or pseudogout since the spectrum of each type of crystal is characteristic. PLM analysis is not definitive since other crystals may also display interference colors. In attestation, one specimen (sample 39, Table I) was likely misdiagnosed by PLM as CPPD due to a morphological similarity between CPPD and another crystal, whereas the original Raman analysis and subsequent analyses ruled out this diagnosis and pointed to an unknown type of crystal. It is important to emphasize that using both methods for a given clinical sample would reduce the error rate in diagnosis. For instance, in one

case (sample 2, Table I) Raman indicated pseudogout, whereas PLM indicated gout. This discrepancy led to a secondary inspection that revealed that this particular patient had both crystals at low concentration. It should be stated that every time Raman indicated that there was a specific crystal present, it turned out that the diagnosis was correct (as per secondary confirmations upon disagreement between PLM and Raman). As shown in the results, the signature peak of BCP (i.e., hydroxyapatite), the third most frequently observed joint crystal, did not overlap with MSUM and CPPD and accordingly BCP may be detected by the proposed approach. Other crystals such as calcium oxalate or cholesterol also have Raman active vibrations.

In conclusion, the current study investigated the detection limit of MSUM and CPPD crystals and diagnosis of gout and pseudogout by Raman spectroscopy. A clinical sample preparation protocol was developed to digest the organics and concentrate the crystals in centrifuge tubes for point-and-shoot Raman detection. The general agreement between PLM and Raman (32 out of 35) in the overall sample pool is misleading in the sense that the diagnoses disagreed in 30% of the diseased samples. This degree of disagreement underlines the need to translate alternative and/or complementary diagnostic methods to PLM for identification of gouty crystal species in the clinic. The proposed sample preparation protocol makes crystal detection easier, which would potentially enable measurements via lower fidelity affordable Raman devices as opposed to expensive research grade instruments. Given that the Raman analysis had a good threshold of detection, that its diagnosis is definitive, and that it is objective, it needs to be assessed on a larger clinical sample set to derive a refined estimate of sensitivity and specificity.

## ACKNOWLEDGMENTS

This publication was made possible by Grant Number R21AR052629 (O.A.) from the National Institute of Arthritis and Musculoskeletal and Skin Diseases division of the NIH. We thank Do-Gyoon Kim, Janardhan Yerramshetty, Debra Bowen, and Judy McVettie for their help with sample collection.

1. P. Dieppe and A. Swan, *Ann. Rheum. Dis.* **58**, 261 (1999).
2. P. Hasselbacher, *Arth. Rheum.* **30**, 637 (1987).
3. H. R. Schumacher, M. S. Sieck, S. Rothfuss, G. M. Clayburne, D. F. Baumgarten, B. S. Mochan, and J. A. Kant, *Arth. Rheum.* **29**, 770 (1986).
4. A. Swan, H. Amer, and P. Dieppe, *Ann. Rheum. Dis.* **61**, 493 (2002).
5. J. B. Segal and D. Albert, *Arthritis Care and Research* **12**, 376 (1999).
6. N. Moradi-Bidhendi and I. G. Turner, *J. Mater. Sci., Mater. Med.* **6**, 51 (1995).
7. C. Gordon, A. Swan, and P. Dieppe, *Ann. Rheum. Dis.* **48**, 737 (1989).
8. S. Honig, P. Gorevic, S. Hoffstein, and G. Weissmann, *Am. J. Med.* **63**, 161 (1977).
9. O. Lazcano, C. Y. Li, R. V. Pierre, J. D. Oduffy, R. S. Beissner, and P. C. Abell-Aleff, *Am. J. Clin. Path.* **99**, 90 (1993).

10. A. J. Swan, B. R. Heywood, and P. A. Dieppe, *J. Rheum.* **19**, 1763 (1992).
11. J. M. Eisenberg, H. R. Schumacher, P. K. Davidson, and L. Kaufmann, *Arch. Int. Med.* **144**, 715 (1984).
12. N. McGill, P. A. Dieppe, M. Bowden, D. J. Gardiner, and M. Hall, *Lancet* **337**, 77 (1991).
13. Y. M. Maugars, L. F. Peru, B. el Messaoudi, G. O. Michaud, J. M. M. Berthelot, A. M. Prost, and G. Daculsi, *J. Rheum.* **21**, 573 (1994).
14. S. R. Hawi, K. Nithipatikom, E. R. Wohlfeil, F. Adar, and W. B. Campbell, *J. Lipid Res.* **38**, 1591 (1997).
15. D. J. McCarty and J. S. Faires, *Curr. Ther. Res., Clin. Exp.* **5**, 284 (1963).
16. M. Pouliot, M. J. James, S. R. McColl, P. H. Naccache, and L. G. Cleland, *Blood* **91**, 1769 (1998).
17. A. G. Fam, H. R. Schumacher, G. Clayburne, M. Sieck, N. S. Mandel, P. T. Cheng, and K. P. H. Pritzker, *J. Rheum.* **19**, 780 (1992).
18. V. R. Kodati, A. T. Tu, and J. L. Turumin, *Appl. Spectrosc.* **44**, 1134 (1990).
19. K. Miura, H. Fukuda, H. Mineta, K. Yamaguchi, H. Harada, H. Yusa, and Y. Tsutsui, *Pathol. Int.* **50**, 992 (2000).
20. J. T. Scott, *Lancet* **1**, 1138 (1983).